Published in final edited form as:
Conf Proc IEEE Eng Med Biol Soc. 2018 July ; 2018: 3766–3796. doi:10.1109/EMBC.2018.8513348.

Predicting beta bursts from local field potentials to improve closed-loop DBS paradigms in Parkinson's patients

Eduardo Martin Moraud[#],
Medical Research Council Brain Network Dynamics Unit, University of Oxford, Oxford, UK, and with the Nuffield Department of Clinical Neurosciences, John Radcliffe Hospital, University of Oxford, Oxford, UK

Gerd Tinkhauser[#],
Medical Research Council Brain Network Dynamics Unit, University of Oxford, Oxford, UK, and with the Nuffield Department of Clinical Neurosciences, John Radcliffe Hospital, University of Oxford, Oxford, UK; Department of Neurology, Bern University Hospital and University of Bern, Bern, Switzerland

Mayank Agrawal,
Swarthmore College, PA, USA

Peter Brown[#], and
Medical Research Council Brain Network Dynamics Unit, University of Oxford, Oxford, UK, and with the Nuffield Department of Clinical Neurosciences, John Radcliffe Hospital, University of Oxford, Oxford, UK

Rafal Bogacz[#]
Medical Research Council Brain Network Dynamics Unit, University of Oxford, Oxford, UK, and with the Nuffield Department of Clinical Neurosciences, John Radcliffe Hospital, University of Oxford, Oxford, UK

[#] These authors contributed equally to this work.

Abstract

Motor symptoms in Parkinson's disease (PD) correlate with an excess in synchrony in the beta frequency band (13-30Hz) of local field potentials recorded from basal ganglia circuits. Recent results have suggested that this abnormal activity arises as a result of changes in specific dynamical features of the underlying neural signatures. In particular, patterns of activity in the beta band have been shown to be structured in bursts of longer durations and higher amplitudes in untreated patients with PD. Closed-loop deep brain stimulation (DBS) paradigms that specifically target these pathological bursts of activity hold promises to help trim, and thus normalize, their abnormal behavior in real-time. Here, we developed classification algorithms that predict pathological beta bursts based on ongoing changes in LFP frequency dynamics. We then compared simulations of prediction-based DBS profiles with existing 'adaptive DBS' alternatives. We show that model-driven stimulation profiles are more precise in restricting the delivery of stimulation to bursts that are considered pathological, while preserving physiological ones. The overall

corresponding author: rafal.bogacz@ndcn.ox.ac.uk.

Europe PMC Funders Author Manuscripts

stimulation time required is also diminished, thus supporting longer battery life. These results represent a conceptual and algorithmic framework for the development of more precise DBS strategies that are selectively tailored to the electrophysiological profile of each patient.

Europe PMC Funders Author Manuscripts

I Introduction

For decades, deep brain stimulation (DBS) therapies have been employed to alleviate motor symptoms in patients suffering from Parkinson's disease (PD) with impressive results [1,2]. The gold standard for such therapies in PD involves applying continuous electrical pulses at high-frequency (130Hz) to specific structures in the basal ganglia, commonly the subthalamic nucleus (STN) or internal globus pallidus (GPi). Electrical neuromodulation of such networks suppresses the excessive levels of synchrony that emerge in local and neighboring circuits, and alleviate motor deficits such as rigidity, tremor or bradykinesia [3,4].

Clinical advances in the use of neural implants for electrical neuromodulation of dysfunctional circuits have concurrently afforded the opportunity to probe the function of these circuits [5,11]. Recoding of local field potentials (LFPs) from DBS electrodes has become a common practice in multiple centers worldwide [6]. This practice has widened our understanding of the neural signatures and mechanisms underlying basal ganglia activity, both at rest and during movement [7], and helped uncover biomarkers that can capture pathological synchrony. In particular, neural correlates of motor symptoms in PD have been consistently associated with abnormal oscillatory patterns in the beta band (13-30Hz) of LFPs [3,4]. These findings have guided the development of the first-generation closed-loop DBS strategy (termed 'adaptive DBS', aDBS), which employs continuous feedback of beta amplitude to activate or deactivate stimulation in real-time whenever the envelope of beta amplitude crosses a fixed threshold [7,8]. Thus far, this threshold has been empirically defined, and manually optimized with respect to the patient's own LFP dynamics.

Recent studies focused on the dynamical differences in beta oscillatory patterns in PD. Comparisons in patients ON *vs.* OFF dopaminergic medication, or ON *vs.* OFF aDBS have revealed significant changes in the temporal organization of beta oscillations [9,10], in particular with regards to their bursting activity patterns. Unlike physiological oscillations that exhibit bursts of short durations (<150ms), PD patients additionally exhibit bursts of long duration and the incidence of these positively correlates with motor symptoms. This suggests that neuromodulation strategies might selectively target such long-duration bursts, and spare those that do not evolve into a pathological state [11]. This observation motivates the development of predictive algorithms that can help predict and specifically target pathological patterns of bursting activity.

Here we developed a computational framework to predict the temporal occurrence of abnormal beta bursts. We developed classification algorithms to estimate the likelihood of upcoming LFPs to evolve into a pathological state, and we compared prediction-driven DBS profiles with existing aDBS strategies. We hypothesized that additional frequency and/or temporal components might convey information to help predict such pathological bursts. Our results show that model-driven DBS strategies are more specific and require less

stimulation time overall. They also allow us to propose a principled approach to determining the optimal threshold for burst-oriented real-time DBS paradigms.

II Methods

LFPs were recorded in two patients (age S1=67, S2=63; disease duration in years: S1=16, S2=5; UPDRS OFF/ON: S1=46.5/25.5, S2=14.5/11) undergoing STN DBS surgery. DBS electrodes (type 3389 Medtronic, USA) were temporarily externalized prior to the connection of the implantable pulse generator. LFPs were recorded using a bipolar contact setup and sampled at 1000Hz (Fig. 1A). Signals were amplified and filtered at 1–250Hz using a custom-made, high-impedance amplifier (with a front-end stage INA128 instrumentation amplifier, Texas Instruments) and recorded through a 1401 analogue/digital converter (Cambridge Electronic Design) on a computer using Spike2. Data from these patients were reported previously [14].

A Data preparation

Pathological bursts of oscillatory activity in the beta band were defined by thresholding (th_1 =75th percentile amplitude) the envelope of the Hilbert Transform of the beta signal (determined as the band-pass filtered signal in the band covering +/3 Hz around the maximum difference in the power spectrum between ON and OFF medication for each electrode [9]: ~13Hz for S1, and ~17Hz for S2) (Fig. 1A-B). Only bursts of durations longer than 200ms were preserved. Shorter ones were discarded under the assumption that they correspond to natural physiological signatures of neural processing. Consecutive bursts with inter-burst intervals shorter than 20ms (~ half a period) were merged together. For each burst retained, its 'onset' was defined as the time from crossing the median to crossing th_1. Table 1 reports the statistics of pathological bursts *vs.* short bursts for each contact pair.

We then parameterized the raw LFPs (subsampled every 50ms) into key features able to capture dynamical changes in the signal. For each sample, we chose a window of 300ms preceding it, and extracted frequency and temporal features. To account for dynamical changes, we split the 300ms window into four consecutive sub-windows of 175ms each with 75% overlap, and we concatenated the corresponding power spectra (from 1Hz to 100Hz) so as to generate a feature vector ζ of 400 dimensions (Fig. 1C).

To account for highly correlated frequency dimensions, we reduced the dimensionality of our input space using PCA and kept features explaining up to 99.5% of the variance (i.e., S1:30 Dimensions, S2: 55 Dimensions).

B Class definition and decoder training

We employed the previous definition of beta bursts to define 2 classes, either C1 corresponding to samples of pathological beta bursts including their ‘onset’, or C0 for the rest (Fig. 2). In order to predict the occurrence of bursts of abnormal bursting activity, we trained classification algorithms (regularized Linear Discriminant Analysis, LDA) for each contact pair, and we tested their performance when decoding the state of each sample using 10-fold cross-validation (N_{train} ~ 4000 samples) (Fig. 2A).

C Measures of performance & comparison to aDBS

To evaluate the accuracy and relevance of prediction-driven DBS profiles, we compared their selectivity with respect to existing aDBS strategies. We simulated the activations A_k that would be generated according to aDBS algorithms as implemented in [7] (i.e. by thresholding the envelope of the beta signal with respect to its median value, including a ramping up/down time of 250ms added onto the ON/OFF logic) (Fig. 3A). We then evaluated the error e with respect to an 'ideal' stimulation pattern I_k that only targets pathological beta bursts i.e. C1. The calculation of the error measure is given as: $e = \sum_{k=1}^{N} (I_k - A_k)^2$ where I_k and $A_k \in [0\ 1]$. Additionally, we quantified the percentage of pathological bursts and of short bursts being targeted by DBS, along with the total stimulation time. Finally, we used our error estimates to determine the threshold for aDBS that optimally and most selectively targeted long duration beta bursts (Fig. 4D).

III Results

A Predictive accuracy

ROC curves for each pair of bipolar electrodes highlighted accurate classification between the two classes, with AUC ranging from 83% to 90% for S1 (Fig. 2B-C), and 71% to 77% for S2. Note that C0 (non-bursting class) included not only periods of low oscillatory activity in the LFP, but also short bursts, and segments of the signal that exceeded the median of the envelope but did not reach the upper threshold th_1. These would ordinarily trigger very brief stimulation during threshold-crossing aDBS.

B Contribution of each frequency band

In order to get further insight into the contribution of each frequency component for distinguishing pathological bursts from other events, we analyzed the factor loadings of each frequency band (in steps of 5Hz) along the principal LDA dimension. Unsurprisingly, the biggest contribution arose from frequencies around the beta band (Fig 3). Nevertheless, albeit comparatively small, additional frequencies all along the power spectrum provided additional information, dynamically changing for the different sub-windows considered.

C Stimulation selectivity

Motivated by the previous results, we simulated the DBS profiles that would result from such predictions. We defined a pair of threshold values [th_{p1} th_{p2}] defining the triggering times of DBS (whenever the probability of C1 exceeded th_{p1} or feel under th_{p2}). These values were optimized offline and converged to a value of 0.5, for which the cumulative error with respect to I_k was $e = 610$ for S1 ($e = 807$ for S2) (Fig. 4C). In contrast for the same LFP signal, aDBS patterns (triggered exclusively based on the median of the envelope) led to significantly bigger errors ($e = 717$ for S1, $e = 1118$ for S2). In particular, additional errors resulted predominantly from stimulating short bursts (assumed to be non-pathological), and periods of beta activity just above the median. As a result, aDBS required markedly longer stimulation time overall (Fig. 4B).

Europe PMC Funders Author Manuscripts

D Optimizing 'aDBS'

We finally aimed to obtain comprehensive comparisons with an optimized version of aDBS, in which the threshold value that triggers stimulation (its only degree of freedom) would be tuned for the specific dynamical characteristics of each LFP. For each set of electrodes, we systematically mapped the error *e* for all threshold values in the range [0.5 - 0.95], and we selected the one minimizing that measure (~0.7 for S1 and ~0.8 for S2) (Fig. 4D). We then compared the resulting patterns with prediction-based counterparts. In this framework, both algorithms performed very similarly according to all measures analyzed, suggesting a highly predominant contribution of beta oscillations in the definition and prediction of pathological bursts.

IV Conclusion

Deep Brain Stimulation is a well-established neuromodulation technique to alleviate motor symptoms in PD. To date, DBS has only been applied continuously, in part due to a lack of mechanistic understanding of the underlying pathological neural processes and to technical requirements. Albeit highly efficacious, continuous stimulation is inherently expensive in terms of battery life. It is also suboptimal to address ongoing patient-specific neural requirements, and often limited by stimulation-induced side effects. Recent clinical experiments show that non-continuous 'aDBS' strategies, which adapt in real-time based on feedback of beta amplitude, are at least as successful in alleviating motor symptoms, but require considerably less stimulation time. Non-continuous approaches also hold promises to help minimize undesired side effects that result from DBS [12,13].

Here, we aimed to refine closed-loop strategies by developing classification-based algorithms that capture and selectively target pathological dynamics. We showed that model-driven algorithms that trigger DBS based on ongoing predictions of such abnormal beta bursts are more selective, and in turn require less stimulation time than threshold-crossing driven aDBS. From an implementation standpoint, the developed approach is simple, requires few samples for training classification models, and may be iteratively updated throughout an experiment to account for time-varying changes in neural dynamics.

A Future perspectives

A main conceptual limitation of the presented methodology is the underlying assumption that *pathological* beta bursts correspond to those exhibiting lengths above a given duration (assumed 200ms [9–10]). While strong correlations were reported in such studies between the duration of beta bursts and motor symptoms in PD, a causal link is still missing. In this regard, the presented methodology may provide a technical framework to validate the link between beta burst duration, targeted DBS and motor control. Moreover it can be updated in the future with new knowledge of beta signal dynamics in PD

Additionally, our methodology is built around the hypothesis that multiple frequencies in the power spectrum (and their temporal dynamics) may provide meaningful information in helping predict the occurrence of pathological bursts. Our results emphasize that despite the addition of multiple frequency bands, it is still beta oscillations which provide the main

source of separation between classes. Further analysis with smaller time-scales might help pinpoint frequency changes throughout bursts, and time-specific contributions not accounted for in our broad analyses. However, perhaps the most immediate impact of the proposed framework is the provision of a simple and principled way in which to optimize the threshold used in real-time aDBS that takes in to account the LFP dynamics within each patient.

Acknowledgments

Research supported by Grant numbers MC_UU_12024/5 and MC_UU_12024/1 of the Medical Research Council, UK. GT received financial support from the Swiss Parkinson Association, Switzerland.

References

[1]. Deuschl G, et al. A randomized trial of deep-brain stimulation for Parkinson’s disease. N Engl J Med. 2006; 355:896–908. [PubMed: 16943402]

[2]. Strauss I, Kalia SK, Lozano AM. Where are we with surgical therapies for Parkinson's disease? Parkinsonism & related disorders. 2014; 20:187–191.

[3]. Hammond C, Bergman H, Brown P. Pathological synchronization in Parkinson's disease: networks, models and treatments. Trends in neurosciences. 2007; 30:357–364. [PubMed: 17532060]

[4]. Ashkan K, Rogers P, Bergman H, Ughratdar I. Insights into the mechanisms of deep brain stimulation. Nature Reviews Neurology. 2017; 13:548–554. [PubMed: 28752857]

[5]. Hammond C, Bergman H, Brown P. Pathological synchronization in Parkinson's disease: networks, models and treatments. Trends in neurosciences. 2007; 30:357–364. [PubMed: 17532060]

[6]. Lozano AM, Lipsman N. Probing and regulating dysfunctional circuits using deep brain stimulation. Neuron. 2013; 77:406–424. [PubMed: 23395370]

[7]. Little S, Pogosyan A, Neal S, Zavala B, Zrinzo L, Hariz M, Foltynie T, Limousin P, Ashkan K, Fitzgerald J, Green AL, et al. Adaptive Deep Brain Stimulation in Advanced Parkinson’s disease. Annals Neurology. 2013; 74:449–457.

[8]. Little S, Beudel M, Zrinzo L, Foltynie T, Limousin P, Hariz M, Neal S, Cheeran B, Cagnan H, Gratwicke J, Aziz TZ, et al. Bilateral Adaptive Deep Brain Stimulation is effective in Parkinson’s Disease. Journal of Neurology and Neurosurgery. 2015

[9]. Tinkhauser G, Pogosyan A, Little S, Beudel M, Herz DM, Tan H, Brown P. The modulatory effect of adaptive Deep Brain Stimulation on Beta Bursts in Parkinson’s disease. Brain. 2017a; 140:1053–1067. [PubMed: 28334851]

[10]. Tinkhauser G, Pogosyan A, Tan H, Herz DM, Kuhn AA, Brown P. Beta Burst Dynamics in Parkinson’s Disease ON and OFF dopaminergic medication. Brain. 2017a; 140:2968–2981. [PubMed: 29053865]

[11]. Ramirez-Zamora A, et al. Evolving Applications, Technological Challenges and Future Opportunities in Neuromodulation: Proceedings of the 5th Annual Deep Brain Stimulation Think Tank. Frontiers in Neuroscience. 2018; 11:1–25.

[12]. Little S, Tripoliti E, Beudel M, Pogosyan A, Cagnan H, Herz D, et al. Adaptive deep brain stimulation for Parkinson’s disease demonstrates reduced speech side effects compared to conventional stimulation in the acute setting. J Neurol Neurosurg Psychiatry. 2016b; 87:1388–9. [PubMed: 27530809]

[13]. Rosa M, Arlotti M, Marceglia S, et al. Adaptive deep brain stimulation controls levodopa-induced side effects in Parkinsonian patients. Mov Disord. 2017; 32:628–9. [PubMed: 28211585]

[14]. Kühn AA, Kupsch A, Schneider GH, Brown P. Reduction in subthalamic 8-35 Hz oscillatory activity correlates with clinical improvement in Parkinson’s disease. Eur J Neurosci. 2006; 23:1956–1960. [PubMed: 16623853]

Europe PMC Funders Author Manuscripts

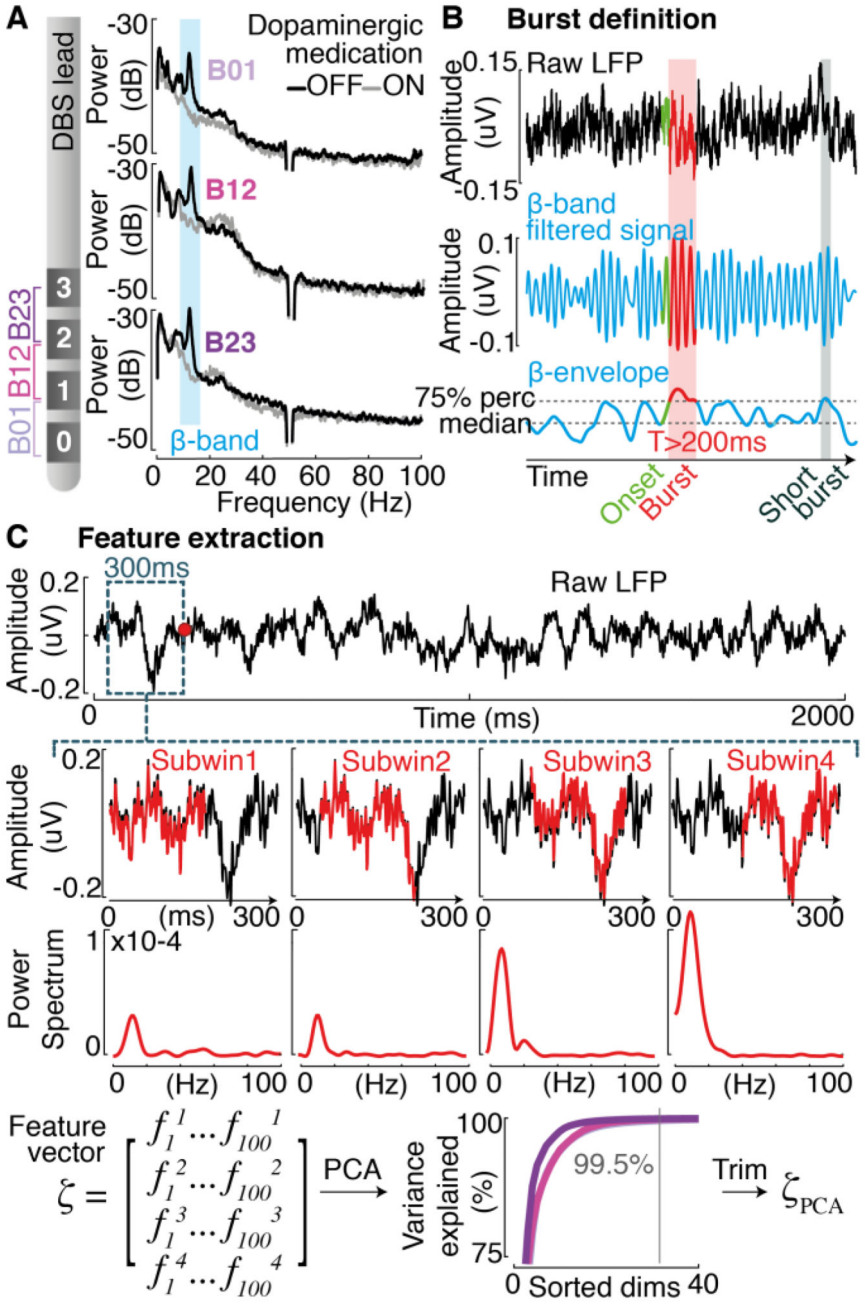

Figure 1.

(**A**) Comparison of power spectrum profiles of LFPs recorded as bipolar signals from consecutive pairs of electrodes from a DBS lead for patient S1, either 'ON' dopaminergic medication (gray traces) or 'OFF' (black). The beta band is derived as +/-3 Hz around the peak distinguishing both conditions (cyan). (**B**) Definition of beta bursts: The envelope of the beta signal is thresholded at the 75% percentile amplitude. Only bursts of durations exceeding 200ms are defined as pathological. (**C**) Parameterisation: For each sample (every 50ms), frequency components are calculated over a window of 300ms. The feature vector is

composed of spectral values over moving subwindows (175ms, 75% overlap). PCA is applied to reduce the dimensionality (99.5% of the variance).

Europe PMC Funders Author Manuscripts

Europe PMC Funders Author Manuscripts

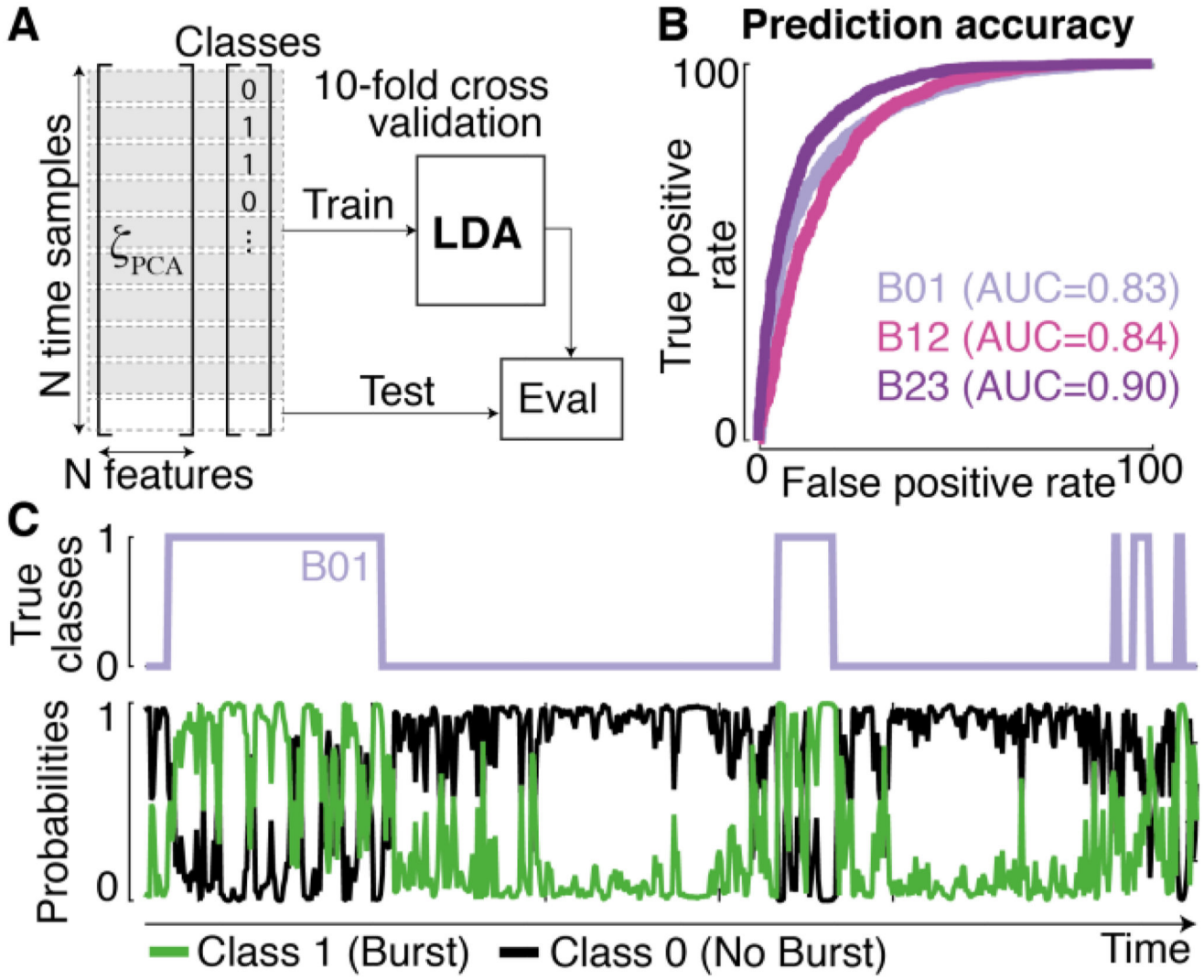

Figure 2.

(**A**) Classification methodology. Feature vector comprising frequency changes preceding each time sample and binarized classes (burst *vs.* no burst) are employed to train and test an LDA classifier. Accuracy is validated using 10-fold cross-validation (**B**) ROC curves for each pair of bilateral electrodes for subject S1 (**C**). Example traces of true class definition for one contact pair and prediction probabilities for each class.

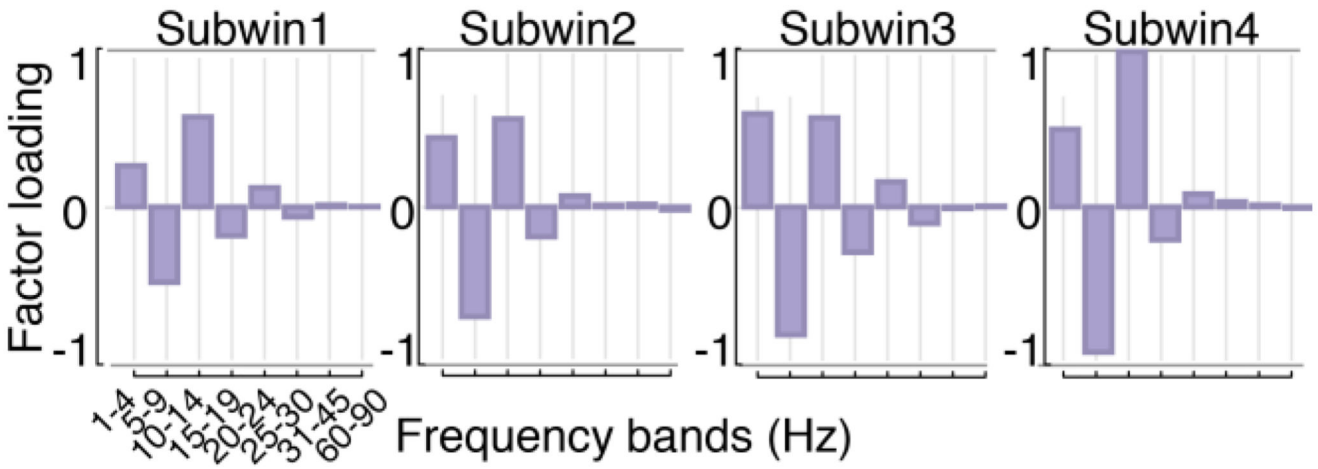

Figure 3.
Contribution of each frequency band to the principal LDA dimension separating the two classes C1 and C0 for S1 B01 (steps of 5Hz).

Europe PMC Funders Author Manuscripts

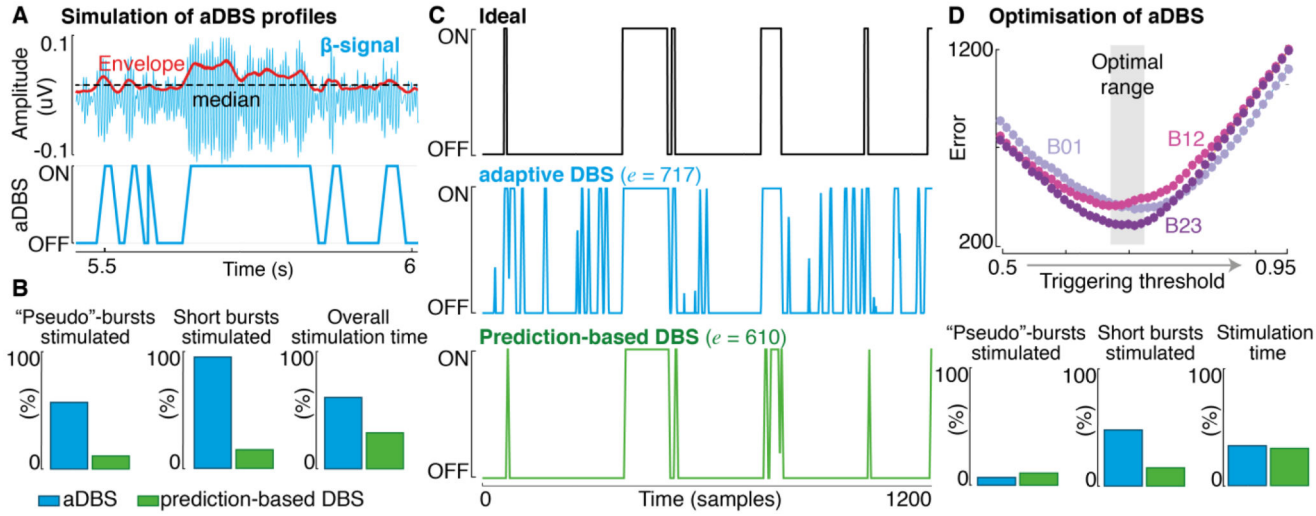

Figure 4.

Comparison of aDBS and prediction-based DBS profiles for S1. (**A**) Simulation of aDBS traces for an illustrative LFP trace. (**B**) Percentage of short bursts, "pseudo"-bursts (segments of signal above the median, but never reaching the upper threshold), and overall stimulation time required for each method for contact B01. (**C**) Profiles for the ideal, aDBS and predictive-based DBS, and cumulative errors. (**D**) Optimisation of aDBS algorithms for different thresholds and related statistics (same as panel B).

Europe PMC Funders Author Manuscripts

Europe PMC Funders Author Manuscripts

electrode pair		Long ('Pathological')		Short	
		# bursts per sec	Mean duration (ms)	# bursts per sec	Mean dur (ms)
S1	B01	0.37	722.8 +/- 54.4	0.45	107.3 +/- 4.8
	B12	0.38	775.6 +/- 68.6	0.34	102.6 +/- 5.9
	B23	0.26	1106 +/- 179	0.25	109.0 +/- 6.3
S2	B01	0.86	403.3+/-20.0	1.34	81.8+/-2.9
	B12	0.84	397.9+/-24.8	1.32	88.0+/-2.9
	B23	0.77	356.3+/-15.8	1.62	90.0+/-2.6